Journal of Power Sources 196 (2011) 5674–5678

Contents lists available at ScienceDirect

Journal of Power Sources

journal homepage: www.elsevier.com/locate/jpowsour

Short communication

Investigation of the rechargeability of Li–O_2 batteries in non-aqueous electrolyte

Jie Xiao*, Jianzhi Hu, Deyu Wang, Dehong Hu, Wu Xu, Gordon L. Graff, Zimin Nie, Jun Liu, Ji-Guang Zhang[1]

Pacific Northwest National Laboratory, Energy and Environment Directorate, Richland, WA 99352, USA

ARTICLE INFO

Article history:
Received 21 December 2010
Accepted 18 February 2011
Available online 26 February 2011

Keywords:
Li–air batteries
Carbon air electrode
Oxygen diffusion
Energy storage

ABSTRACT

To understand the limited cycle life performance and poor energy efficiency associated with rechargeable lithium–oxygen (Li–O_2) batteries, the discharge products of primary Li–O_2 cells at different depths of discharge (DOD) were systematically analyzed using XRD, FTIR and Ultra-high field MAS NMR. When discharged to 2.0 V, the reaction products of Li–O_2 cells include a small amount of Li_2O_2 along with Li_2CO_3 and RO–(C=O)–OLi in the alkyl carbonate-based electrolyte. However, regardless of the DOD, there is no Li_2O detected in the discharge products in the alkyl-carbonate electrolyte. For the first time it was revealed that in an oxygen atmosphere the high surface area carbon significantly reduces the electrochemical operation window of the electrolyte, and leads to plating of insoluble Li salts on the electrode at the end of the charging process. Therefore, the impedance of the Li–O_2 cell continues to increase after each discharge and recharge process. After only a few cycles, the carbon air electrode is completely insulated by the accumulated Li salt terminating the cycling.

Published by Elsevier B.V.

Li-ion batteries remain the most promising energy-storage technology for deployment in hybrid electric vehicles (HEVs) and electric vehicles (EVs), which are being promoted to replace traditional vehicles equipped with internal combustion engines [1]. Although existing Li-ion batteries may satisfy the need for short-range Plug-in HEVs, applications of EVs will require energy-storage systems with increased energy densities. Among the various electrochemical couples investigated in this field, Li–O_2 batteries have the largest theoretical specific energy. The cathode material, oxygen, is stored in the surrounding environment and can be absorbed into the Li-air cell during the discharge process.

Previous work [2–4] indicated that the performance of Li–O_2 batteries is significantly affected by several factors, including the pore size and volume of carbon [5], the electrolyte [6–8], the binder [4], the O_2 partial pressure [3], and the air-breathing water barriers [9,10]. Unlike Li-ion batteries operating in a nearly O_2-free environment, the carbon electrode, the electrolyte, and even the discharge products of Li–O_2 batteries are exposed to the O_2 environment, which may become unstable during long-term operations [11,12]. Although several research groups have documented that Li–O_2 batteries can be recharged [13–17], most of these groups assumed that the reaction product produced during discharge is primarily Li_2O_2, which can be recharged to Li and O_2. Recently, Mizuno et al. [18] used FTIR spectra to investigate the discharge products of Li–O_2 batteries with a propylene carbonate (PC)-based electrolyte and a MnO_2 catalyst. They found that the discharge products were carbonates lithium alkyl carbonate and/or Li_2CO_3 without any desired Li_2O_2. However, the reason of the formation of dominant Li_2CO_3 instead of Li_2O_2 or Li_2O stays unclear.

In this paper, we report our recent studies of the reaction products of Li–O_2 batteries and relate the formation of Li_2CO_3 to similar phenomena found in leaking lithium batteries reported in the early date. The combined effects of carbon, electrolyte, and their interactions under an oxygen atmosphere on the final reaction products at the end of both charge and discharge processes have been investigated systematically. The critical factors to make a Li–O_2 rechargeable are also discussed in this work.

1. Experimental

The Ketjenblack (KB)-based air electrodes used in this study were prepared as described in our previous publication [19]. The weight ratio of carbon/Teflon after drying was 85:15. The final loading of carbon in the electrode was controlled at 15.1 mg cm^{-2}. The Li–air coin cells (type 2325 coin cell kits from CNRC, Canada) were assembled in an argon-filled glove box (MBraun Inc.) with the moisture and oxygen contents less than 1 ppm. Nineteen evenly spaced holes were machined into the positive pans of the 2325 coin cells to allow air passage [19]. Lithium disks (1.59 cm in diameter and 0.5 mm thick) were used as the anodes. The electrolyte was prepared by dissolving 1 mol lithium bis(trifluoromethanesulfonyl)imide (LITFSI) in ethylene carbonate

* Corresponding author. Tel.: +1 509 3754598; fax: +1 509 3753864.
E-mail addresses: jie.xiao@pnl.gov (J. Xiao), jigunag.zhang@pnl.gov (J.-G. Zhang).
[1] Tel.: +1 509 3726515; fax: +1 509 3753864.

0378-7753/$ – see front matter. Published by Elsevier B.V.
doi:10.1016/j.jpowsour.2011.02.060

(EC)/propylene carbonate (PC) (1:1 weight ratio). The salts and solvents used in the electrolyte were all battery grade materials from Ferro Corp. A Whatman GF/D glass microfiber filter paper (1.9 cm diameter) was used as the separator. The coin cells were placed in a Teflon container filled with pure O_2. The electrochemical tests were performed at room temperature using an Arbin BT-2000 battery tester. A current density of 0.1 mA cm^{-2} was used for all the tests. Cells used for characterization of discharge products were discharged to 2.0 V and then held at 2.0 V until the current density decreased to less than $I/5 = 0.02$ mA cm^{-2}. To evaluate rechargeability, cells were tested between 2.0 and 4.4 V without holding at the cut-off voltages. Cyclic voltammetry (CV) tests were used to determine the stabilities of the electrolyte and the batteries with or without O_2. A CHI 660C electrochemical analyzer (CH instrument) was used for the CV tests. The cells (in Teflon containers filled with O_2) were scanned between 2.0 V and 4.4 V at a rate of 0.1 mV s^{-1} in an argon or a pure O_2 atmosphere. The alternating current (AC) impedances of the cells were measured using a CHI 660C electrochemical analyzer operating in the frequency range of 0.01–10^6 Hz with an AC voltage amplitude of 5 mV.

The structures of the discharged products were characterized using a Philips X'Pert X-ray diffractometer in a θ–2θ scan mode and Cu Kα radiation at $\lambda = 1.54$ Å. All samples were scanned at 0.5° min^{-1} between 10° and 80°. The FTIR measurements were performed using a Bruker Optics Vertex 70 FTIR spectrometer at a resolution of 4 cm^{-1} and within the range 4000 cm^{-1} and 400 cm^{-1}. The ultra-high-field ^{6}Li MAS NMR experiments were performed on a Varian-Oxiford Inova 63 mm widebore 900 MHz NMR spectrometer. The main magnetic field was 21.1 T and the corresponding ^{6}Li Lamor frequency was 132.531 MHz. A homemade 3.2 mm pencil type MAS probe was used for the ^{6}Li MAS NMR experiments. About 5–8 mg of sample was used for each measurement, and the sample spinning rate was approximately 18 kHz. All the ultra-high-field ^{6}Li MAS NMR spectra were acquired at room temperature and were referenced to 1-M LiCl in H_2O (0 ppm) using solid LiCl (at −1.25 ppm) as a secondary reference. To eliminate the contribution from the electrolytes, both electrodes that were discharged in O_2 and in air were washed with acetonitrile and dried in a vacuum oven overnight prior to the NMR measurements.

2. Results and discussion

To detect the existence of Li_2O_2 and Li_2O in the discharge products the cutoff voltage was extended from 2.0 V to 0.5 V and the reaction products at different DODs analyzed and compared. Fig. 1 shows the XRD patterns of the air electrodes at different DODs in the O_2 atmosphere. The structures of the commercial chemicals Li_2CO_3, Li_2O_2, LiOH, Li_2O, and pure KB-carbon powder also are plotted in Fig. 1 as references. The XRD results show that, when discharged to 2.0 V, Li_2CO_3 coexists with Li_2O_2. For the PC/EC based electrolyte, the decomposition or the formation of the solid electrolyte interface film (SEI) usually begins at around 1.0 V [20], which obviously cannot explain the dominant Li_2CO_3 phase in the cell discharged to 2.0 V. However, as found by Aurbach [12,20] in a leaking Lithium battery, the intermediate product of the reaction between Li and O_2, LiO_2, may react with the carbonate solvent to form Li_2CO_3 because PC/EC is a good substrate for the nucleophilic attack. Part of the intermediate LiO_2 continues to be reduced to Li_2O_2 by accepting another electron and a Li^+ ion. That is, the formation of Li_2CO_3 in the discharge product (≥2.0 V) is from the interaction between LiO_2 and the solvent in the electrolyte. Further discharging the air electrode to below 2.0 V causes severe electrolyte decomposition and the formation of more Li_2CO_3. However, even when discharged to 0.5 V, no Li_2O is detected in the XRD pattern, suggesting that the

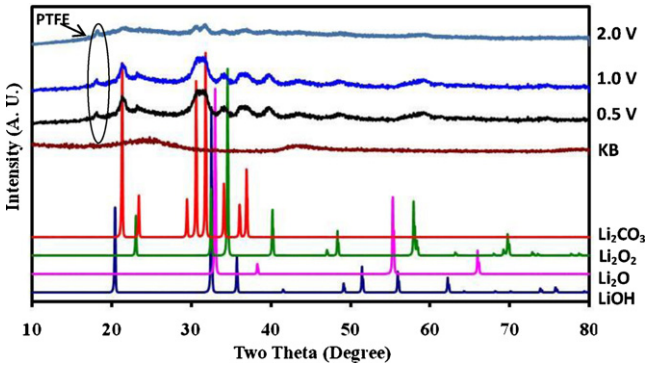

Fig. 1. XRD patterns of the air electrodes discharged at different DOD. For comparison, the chemicals used as standards (i.e., Li_2CO_3, Li_2O_2, Li_2O, and LiOH) also are plotted.

alkyl-carbonate-based electrolyte is not an appropriate medium for the formation of Li_2O.

To confirm the results from the XRD analysis, the discharged air electrodes were further characterized by FTIR spectroscopy as shown in Fig. 2. The peaks at 1630 cm^{-1} and 1247 cm^{-1} correspond to the asymmetric and symmetric stretching of the $-CO_3Li$ group, respectively. The wide band at 1047 cm^{-1} is indicative of the stretching vibration of the C–O band. Thus, an additional compound, lithium alkyl carbonate ($LiRCO_3$), also is identified in the discharged products. The strong bands at 1436 cm^{-1} and 867 cm^{-1} represent the bending of the OCO_2^- group in Li_2CO_3. Both the lithium carbonates and the alkyl carbonates are the products of the interactions between LiO_2 and PC/EC [12]. The amount of $LiRCO_3$ and Li_2CO_3 increases with decreasing voltage because of the increased electrolyte decomposition. The Li–O stretching vibration in Li_2O_2 is seen clearly at 550 cm^{-1} in the air electrode discharged to 2.0 V consistent with the XRD results.

Fig. 3 shows the ultra-high-field MAS ^{6}Li NMR spectra of the air electrodes discharged in different environments. To perform spectral assignments for the various peaks observed in Fig. 3, the spectra for Li_2CO_3, Li_2O_2, LiOH, and Li_2O were acquired as the standards under test conditions that were similar to those used to acquire the spectra for the products of discharge processes. Only the air electrodes discharged to 2.0 V were characterized to confirm our conclusion that a small amount of Li_2O_2 is present even though the intermediate product LiO_2 strongly reacts with the solvents. One of the air electrodes was discharged in pure O_2, and the other one was discharged in ambient air. Based on the observation that the peak centers for both discharged air electrodes (i.e., at −0.15 ppm in O_2 and −0.06 ppm in air) are far away from those of Li_2O (i.e., 2.8 ppm)

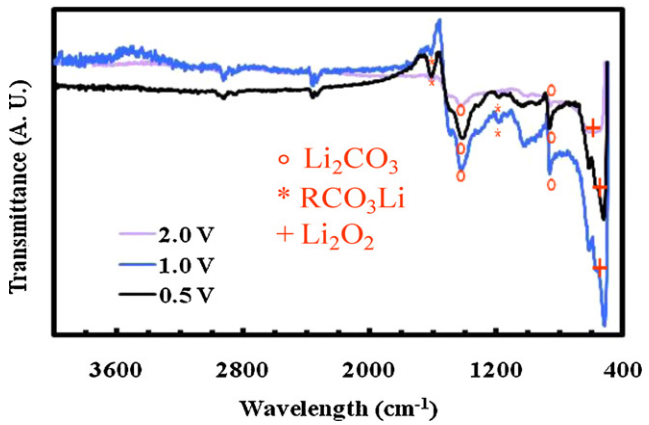

Fig. 2. FTIR spectra of the air electrodes at different DODs.

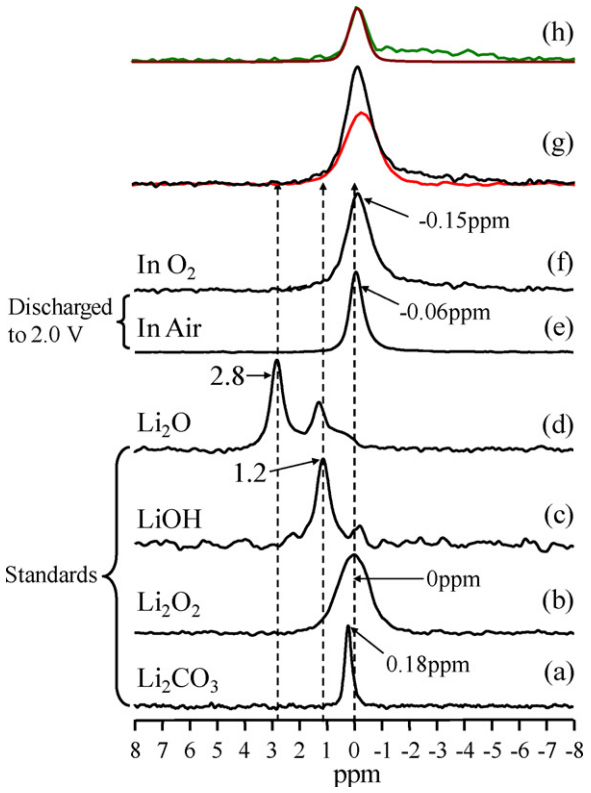

Fig. 3. Ultra-high-field ^{6}Li MAS NMR spectra of the standards (a–d) and the air electrodes discharged in air (e) and O_2 (f). A single-pulse sequence with high power ^{1}H decoupling (~40 kHz) was used for the measurement with a recycle delay time of 70 s and the number of scans varied between 114 and 512 for each spectrum. (g) The superimposed line shapes of (b) (red trace) and (f) (black trace). (h) The difference spectrum resulting in from (g) (green trace) and the simulated line shape (brown) using a line width of 90 Hz. (For interpretation of the references to color in this figure legend, the reader is referred to the web version of the article.)

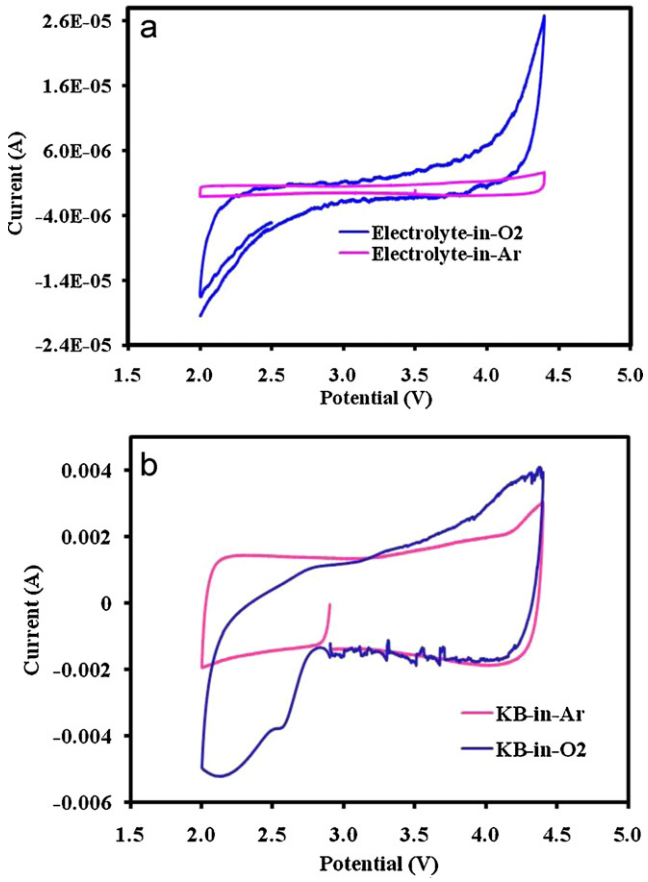

Fig. 4. Cyclic voltammograms of (a) LITFSI (PC/EC) electrolyte without carbon electrode and (b) KB air electrodes in both argon and O_2.

and LiOH (i.e., 1.2 ppm), it can be concluded that neither Li_2O nor LiOH deposited on the carbon surface. However, the peak centers of the two electrodes were very close to both Li_2CO_3 (i.e., 0.18 ppm) and Li_2O_2 (i.e., none detected). It is reasonable to hypothesize that both the Li_2CO_3 and Li_2O_2 structures are present in the discharged electrodes. The line widths of Li_2CO_3 (i.e., 40 Hz) and Li_2O_2 (i.e., 185 Hz) are substantially different because of the different electric-field-gradient (EFG) environment around the Li nucleus [21]. This special feature then was used in Fig. 3 to validate our hypothesis. The line shape of the experimental ^{6}Li MAS NMR spectrum of Li_2O_2 sample was scaled to match that of the experimental spectrum of the electrode discharged in O_2 (see Fig. 3g). Direct subtraction of the two experimental spectra yielded the spectrum shown in Fig. 3h. The line width of the spectrum shown in Fig. 3h (i.e., simulated to be approximately 90 Hz) is significantly less than that of the spectrum for Li_2O_2 (i.e., 185 Hz). This direct and simple subtraction qualitatively confirm our hypothesis that the experimental line shape of the ^{6}Li MAS NMR spectrum of the air electrode consists of components of both Li_2O_2 and Li_2CO_3.

By combining the results from the XRD, FTIR, and ^{6}Li MAS NMR analyses, it can be concluded that, if carbonate-based electrolyte is used in Li–air or Li–O_2 batteries, the main discharge products are Li_2CO_3 and $LiRCO_3$ rather than Li_2O_2. This finding explains the large hysteresis between the charge and discharge curves of a Li–O_2 battery regardless of the current densities.

To further investigate the stability of PC/EC-based electrolyte on the high-surface-area carbon (i.e., 2672 $m^2\ g^{-1}$ for KB carbon) in the O_2 environment, the cyclic voltammograms of the pure electrolyte were measured with and without carbon electrodes in both argon and O_2. These voltammograms are compared in Fig. 4. A flat background was detected for LITFSI in PC/EC under a pure argon atmosphere as shown in Fig. 4a. This result indicates that the electrolyte itself is stable between 2.0 V and 4.4 V. However, when O_2 was introduced the electrochemical window of the electrolyte was shortened as shown in Fig. 4a. When the KB-carbon air electrode was added to the system, the electrolyte becomes much more unstable, even when O_2 is not present. As seen in Fig. 4b, a clear peak occurs at a voltage slightly higher than 4.1 V. This peak is associated with the high surface area of the carbon, which facilitates electrolyte decomposition at high voltages. When the air electrode was scanned in an O_2 atmosphere, a small reduction peak corresponding to the formation of LiO_2 occurred at ~2.6 V, followed by a broad peak corresponding to the further transformation from LiO_2 to Li_2O_2 and Li_2CO_3 between 2.1 V and 2.3 V. It is not surprising that there was no oxidation peak observed in the anodic scan because the oxidation over potential of Li_2O_2 had been pushed to above 4.0 V due to the increased cell resistivity. The broad oxidation peak occurring between 4.0 V and 4.4 V corresponds to decomposition of both the electrolyte and Li_2CO_3/$LiRCO_3$ formed during discharge [22]. It is important to note that the decomposition of Li_2CO_3 does not mean Li_2CO_3 is electrochemically active. During the charging process, carbonates formed during discharging release CO_2 [23], and simultaneously produce other Li salts that coat the carbon surface. In another words, during each cycle, different Li salts are plated at the end of the discharge and charge processes, leading to a significant increase of the impedance of the air electrode.

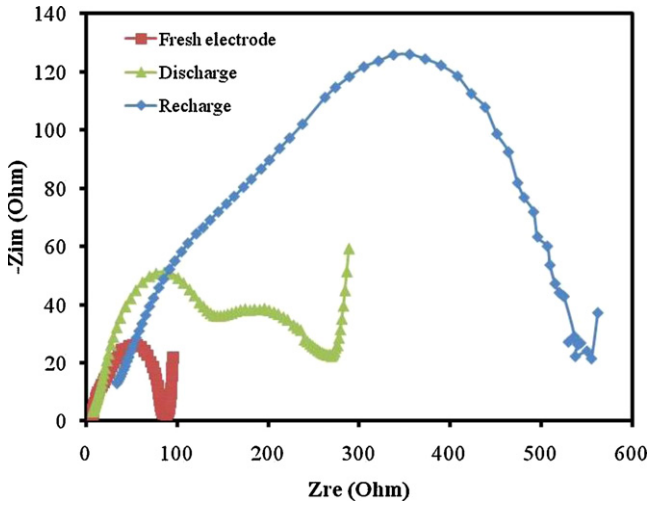

Fig. 5. Nyquist plots of fresh, discharged, and recharged carbon air electrodes.

To further investigate the increase in cell impedance, electrochemical impedance spectroscopy was used to measure the cell impedance for the fresh, discharged, and recharged air electrodes (see Fig. 5). The fresh air electrode exhibits a small semi-circle with a diameter of ~80 Ω at high frequencies in Fig. 5. Because the electrode had not been activated, the diameter of the semicircle reflects the resistance of the SEI layer on the electrode surface. After discharging, two separated semicircles are observed in Fig. 5. The enlarged diameter (200 Ω) of the semi-circle at high frequency is attributed to increased impedance between the SEI layer and the carbon electrode. This is consistent with the formation of Li_2O_2, $LiRCO_3$, and Li_2CO_3 on the surface of the air electrode. After recharging, the resistivity of the air electrode further increases to more than 500 Ω due to the electrolyte decomposition beyond 4.0 V plating more Li salts on the carbon surface.

Fig. 6 shows the typical charge–discharge curves for a KB-carbon-based air electrode operated in an O_2 atmosphere. Even though the discharge voltage limit is set to as high as 2.6 V to minimize electrolyte decomposition, a large polarization was still observed over limited cycles. Based on the above analysis, we concluded that, for a KB-carbon-based air electrode,

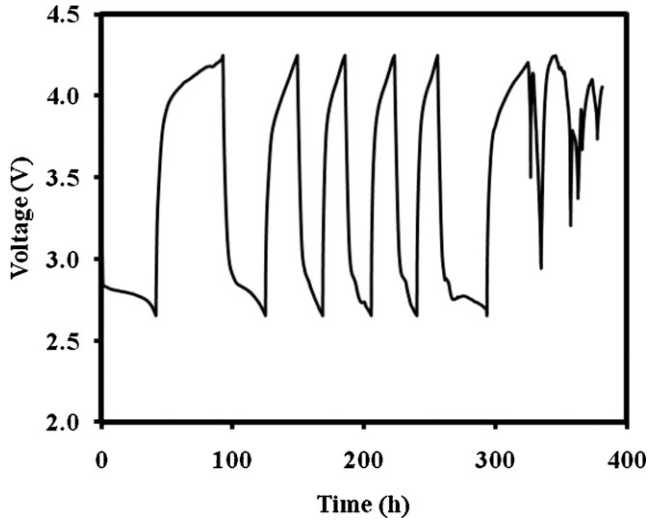

Fig. 6. Cycling ability of Li–O_2 battery using a KB-based air electrode in a LITFSI(PC/EC) electrolyte.

the discharge capacity comes from the formation of Li_2CO_3, along with a small amount of Li_2O_2, while the charge capacity mainly is from the decomposition of Li_2CO_3/$LiRCO_3$ and electrolyte at above 4.0 V. Thus, the Coulombic efficiency of these Li–O_2 cells usually is low. The accumulation of the insulating Li salts accompanied by the continuous consumption of the electrolyte terminates the cycling life of a Li–O_2 battery only after a few cycles.

3. Conclusions

In this study, XRD analysis, FTIR spectroscopy, and ^{6}Li MAS NMR spectroscopy were used to investigate the discharge products of Li–O_2 batteries with alkyl-carbonate electrolytes and KB-carbon-based air electrodes. The analyses found that the primary discharge products are Li_2CO_3 and $LiRCO_3$, with a small amount of Li_2O_2 also present. There was no Li_2O detected regardless of the different DODs. The formation mechanism of Li_2CO_3 and $LiRCO_3$ at 2.0 V was explained through the nucleophilic attack of LiO_2 on the alkylcarbonate solvent. Therefore, it is critical to first identify an appropriate electrolyte in which Li_2O_2 or the intermediate product LiO_2 is stable. Further investigations revealed that the high-surface-area carbon is another key parameter that needs to be modified to achieve rechargeable Li–O_2 batteries because interactions between the electrolyte and the carbon significantly influence the limited electrochemical window of the electrolyte. The repeated coating of different Li salts on the carbon electrode after each discharge and charge process diminishes the electronic conductivity of the air electrode, ultimately leading to failure of Li–O_2 batteries. Future work should focus on identifying an appropriate electrolyte and a carbon with a reduced surface area, as well as a catalyst and an optimized electrode structure that will make Li–O_2 batteries truly rechargeable.

Acknowledgement

This work was supported by the Laboratory Directed Research and Development Program at Pacific Northwest National Laboratory, which is a multiprogram national laboratory operated by Battelle for the U.S. Department of Energy. We acknowledge Ms. Mary Hu and Dr. Ja Hun Kwak for their assistance with the NMR experiments and data analysis.

References

[1] J. Xiao, N.A. Chernova, M.S. Whittingham, Chem. Mater. 20 (2008) 7454.
[2] J. Xiao, W. Xu, D. Wang, J.-G. Zhang, J. Electrochem. Soc. 157 (2010) A294.
[3] J. Read, K. Mutolo, M. Ervin, W. Behl, J. Wolfenstine, A. Driedger, D. Foster, J. Electrochem. Soc. 150 (2003) A1351.
[4] W. Xu, J. Xiao, D. Wang, J. Zhang, J.-G. Zhang, J. Electrochem. Soc. 157 (2010) A219.
[5] K.M. Abraham, Z. Jiang, J. Electrochem. Soc. 143 (1996) 1.
[6] W. Xu, J. Xiao, J. Zhang, D. Wang, J.-G. Zhang, J. Electrochem. Soc. 156 (2009) A773.
[7] W. Xu, J. Xiao, D. Wang, J. Zhang, J.-G. Zhang, Electrochem. Solid-State Lett. 13 (2010) A48.
[8] J. Read, J. Electrochem. Soc. 149 (2002) A1190.
[9] J.-G. Zhang, D. Wang, W. Xu, J. Xiao, R.E. Williford, J. Power Sources 195 (2010) 4332.
[10] D. Wang, J. Xiao, W. Xu, J.-G. Zhang, J. Electrochem. Soc. 157 (2010) A760.
[11] C.O. Laoire, S. Mukerjee, K.M. Abraham, E.J. Plichta, M.A. Hendrickson, J. Phys. Chem. C 113 (2009) 20127.
[12] D. Aurbach, M. Daroux, P. Faguy, E. Yeager, J. Electroanal. Chem. 297 (1991) 225.
[13] Y.C. Lu, H.A. Gasteiger, M.C. Parent, V. Chiloyan, Y. Shao-Horn, Electrochem. Solid-State Lett. 13 (2010) A69.
[14] C. Tran, X.Q. Yang, D. Qu, J. Power Sources 195 (2010) 2057.
[15] D. Zhang, R. Li, T. Huang, A. Yu, J. Power Sources 195 (2010) 1202.
[16] G. Girishkumar, B. McCloskey, A.C. Luntz, S. Swanson, W. Wilcke, J. Phys. Chem. Lett. 1 (2010) 2193.
[17] T. Ogasawara, A. Débart, M. Holzapfel, P. Novák, P.G. Bruce, J. Am. Chem. Soc. 128 (2006) 1390.

[18] F. Mizuno, S. Nakanishi, Y. Lotani, S. Yokoishi, H. Iba, Electrochemistry 78 (2010) 403.
[19] J. Xiao, D. Wang, W. Xu, D. Wang, R.E. Williford, J. Liu, J.-G. Zhang, J. Electrochem. Soc. 157 (2010) A487.
[20] D. Aurbach, H. Gottlieb, Electrochim. Acta 34 (1989) 141.
[21] K.J.D. Mackenzie, M.E. Smith, Multinuclear Solid-State NMR of Inorganic Materials, Pergamon Press, Elsevier Science Ltd., 2002.
[22] W. Xu, V.V. Viswanathan, D. Wang, S.A. Towne, J. Xiao, Z. Nie, D. Hu, J.-G. Zhang, Investigation on the charge processes of Li–O_2 batteries, J. Power Sources 196 (2011) 3894.
[23] G. Gopalakrishnan, B. McCloskey, Symposium on Scalable Energy Storage Beyond Lithium III: Materials Perspectives, Oak Ridge, Tennessee, October 2010, 2010.